



## 23 Introduction

24 Ethanolamine is a very important molecule with a diverse range of applications such as making detergents,<sup>1</sup>  
25 and absorption of CO<sub>2</sub> and other acid gases.<sup>2</sup> Because of its diverse industrial use, ethanolamine is  
26 considered to be a contaminant in soil.<sup>3</sup> In biology,<sup>4,5</sup> ethanolamine is probably best known as a headgroup  
27 in phospholipids.<sup>4</sup> The recent discovery of ethanolamine in space suggests its role in the origin of life to  
28 form early lipids.<sup>6</sup> It is also associated with various diseases such as inflammation<sup>7</sup> and Alzheimer's  
29 disease.<sup>8</sup> Thus, the detection of ethanolamine has attracted the interest of analytical chemists, and  
30 chromatography is the most popular method.<sup>9</sup>

31 Biosensors for ethanolamine have also been developed based on enzyme electrodes.<sup>10</sup> For the  
32 detection of small molecules, DNA aptamers have advantages in excellent binding affinity, specificity,  
33 programmability and ease of modification.<sup>11-14</sup> Among the reported small molecule binding aptamers, the  
34 ones for ethanolamine are very intriguing.<sup>15</sup> Ethanolamine is such a small molecule with only an amine  
35 group and a hydroxyl group that can potentially interact with DNA (e.g., via hydrogen bonding and  
36 electrostatic attraction). Yet, the reported aptamers had much lower dissociation constants (9.6 nM for one  
37 of the original aptamers<sup>16</sup>) compared to most other small molecular binding aptamers (high nM to low  $\mu$ M).  
38 For example, the classic adenosine binding aptamer has a  $K_d$  of  $\sim 6 \mu$ M,<sup>17,18</sup> and a newly selected dopamine  
39 binding aptamer has a  $K_d$  of  $\sim 0.12 \mu$ M.<sup>14,19</sup> These molecules can interact with DNA via  $\pi$ - $\pi$  stacking and  
40 multiple hydrogen bonding interactions, and thus are expected to have stronger affinity compared to  
41 ethanolamine with its aptamers.

42 The ethanolamine aptamers were obtained by immobilization of ethanolamine on magnetic beads  
43 via its amine group (by reaction with either epoxy or tosyl activated magnetic beads).<sup>15</sup> Thus, the exposed  
44 feature is only a hydroxyl group. So far, most of the binding assays and related biosensors involved  
45 immobilized ethanolamine or immobilized aptamers instead of homogeneous assays.<sup>15,16,20-24</sup> We reason  
46 that homogeneous assays are less susceptible to unintended surface/aptamer or surface/target interactions,  
47 which might cause artifacts.<sup>25-27</sup>

48 So far, only two homogeneous assays were reported for the ethanolamine aptamers. One used  
49 thioflavin T (ThT) to stain the aptamers, and ethanolamine was detected by fluorescence quenching.  
50 However, the apparent  $K_d$  was around 40 mM ethanolamine.<sup>28</sup> We reason that the observed quenching was  
51 likely due to other events than aptamer binding (nM  $K_d$  expected). Another homogenous assay labeled the  
52 aptamer with a fluorophore and a quencher to form a molecular beacon structure, where low nM  $K_d$  was  
53 observed by plotting the melting temperature of the DNA and ethanolamine concentration.<sup>29</sup> This assay  
54 indicated binding also to 1  $\mu$ M ethanol or propylamine as well. It's hard to imagine an aptamer can bind

55 ethanol, ethanolamine, and also propylamine, all at low  $\mu\text{M}$  and even nM concentrations, since they are  
56 very different molecules as aptamer targets.

57 Recently, quite a few papers have been published to scrutinize the aptamers for a few some small  
58 molecules such as arsenic, ampicillin, chloramphenicol and a few pesticides,<sup>30-35</sup> where careful  
59 homogeneous binding assays revealed no binding.<sup>36</sup> Given that heterogeneous aptamer binding assays are  
60 more difficult to interpret,<sup>37, 38</sup> and intrigued by the reported binding assays for ethanolamine, in this work,  
61 we examined the binding of the ethanolamine aptamers using homogenous binding assays.

62

## 63 **Materials and Methods**

### 64 **Chemicals**

65 All of the DNA samples were purchased from Integrated DNA Technologies (Coralville, IA, USA), and  
66 their sequences are listed in Table 1. Ethanolamine, thioflavin T (ThT), KCN and Tween 20 were from  
67 Sigma-Aldrich. HEPES (4-(2-hydroxyethyl)-1-piperazineethanesulfonic acid) was obtained from Bio Basic  
68 (Toronto, ON, Canada). Phosphate buffer, KCl, NaCl,  $\text{MgCl}_2$  and  $\text{CaCl}_2$  were obtained from Amerseco.  
69 Gold nanoparticles (AuNPs, 13 nm diameter) were synthesized in our laboratory using the Turkevich  
70 method.<sup>39, 40</sup> Milli-Q water was used to prepare all of the buffers and solutions. The following two buffers  
71 were prepared: Binding Buffer 1 (BB1): 20 mM HEPES, pH 7.6 HEPES, 100 mM NaCl, 5 mM KCl, 2 mM  
72  $\text{MgCl}_2$ , 1 mM  $\text{CaCl}_2$ , 0.02% Tween 20; and Binding Buffer 2 (BB2): 20 mM phosphate buffer pH 7.6, 100  
73 mM NaCl, 5 mM KCl, 2 mM  $\text{MgCl}_2$ , 1 mM  $\text{CaCl}_2$ . These buffers were prepared according to the aptamer  
74 selection condition.<sup>28</sup>

75 **Table 1. The DNA sequence used in this work.**

DNA names	Sequences (from 5' to 3')
EA#14.3K42	ATA CCA GCT TAT TCA ATT TGA GGC GGG TGG GTG GGT TGA ATA
EA#14.3K32	ATA CCA GCT TAT TCA ATT TGA GGC GGG TGG GT
EA-Const	GAG GTG GGT GGG TGG G
C-EA-Const	CCC ACC CAC CCA CCT C
FAM-DNA	AAA AAA AAA CCC AGG TTC TCT-FAM
AS1411	GGT GGT GGT GGT TGT GGT GGT GGT GG
24-mer	ACG CAT CTG TGA AGA GAA CCT GGG

76

## 77 **Isothermal Titration Calorimetry (ITC)**

78 All the ITC experiments were performed on a VP-ITC microcalorimeter instrument (MicroCal). Before  
79 each time experiment, the cell chamber and syringe were cleaned by ethanol and Milli-Q water carefully  
80 followed by washing with BB1 five times. For ethanolamine ITC experiment, 5  $\mu\text{M}$  aptamer (2 mL) was  
81 added into the cell chamber, and 200  $\mu\text{M}$  ethanolamine (280  $\mu\text{L}$ ) was loaded into the syringe. All of  
82 ethanolamine and DNA samples were diluted into BB1. The titrations will carried out at 25°C and each  
83 time 10  $\mu\text{L}$  ethanolamine was injected except for the first time injection (2  $\mu\text{L}$ ). For the DNA to cDNA  
84 control experiment, the cell was loaded into 2  $\mu\text{M}$  (2 mL) EA-Const aptamer and the syringe was loaded  
85 with 5.72 $\mu\text{M}$  (280  $\mu\text{L}$ ) C-EA-Const aptamer.

## 86 **ThT fluorescence spectroscopy**

87 To test the influence of ethanolamine for the fluorescence of ThT/aptamer, 200 nM aptamer in BB1 was  
88 mixed with 10  $\mu\text{M}$  ThT (final volume 0.5 mL in a quartz cuvette). Then a 2 M ethanolamine stock solution  
89 prepared in BB1 was gradually titrated into the quartz cuvette to reach designated concentrations of  
90 ethanolamine. For the low concentration ethanolamine experiment, the only difference was to titrate with  
91 10  $\mu\text{M}$  and 100  $\mu\text{M}$  ethanolamine stock solutions. The fluorescence intensity at 490 nm was measured by  
92 a Variant Eclipse fluorometer with 425 nm excitation.

## 93 **Colloidal stability of AuNPs**

94 To test the influence of ethanolamine to the colloidal stability of AuNPs, different concentrations  
95 ethanolamine up to 5 mM were added into  $\sim 5$  nM AuNPs (100  $\mu\text{L}$  final volume, diluted one time from the  
96 as-synthesized AuNPs). After incubation for 1 min, the UV-vis absorption spectra of the samples were  
97 collected. For determine the degree of aggregation, the extinction ratio of at two wavelengths ( $A_{630}/A_{620}$ )  
98 was used.

## 99 **Influence of ethanolamine on DNA adsorption to AuNPs**

100 Different concentrations ethanolamine (up to 3 mM), 2 nM AuNPs, 100 nM FAM-labeled DNA, 45 mM  
101 phosphate buffer (pH 7.5) and 50 mM NaCl were incubated for 10 min at room temperature. After  
102 centrifugation of the samples centrifuged for 15 min at 15000 rpm, 5  $\mu\text{L}$  of the supernatants were mixed  
103 with 95  $\mu\text{L}$  5 mM pH 7.5 phosphate buffer in a 96-well microplate for fluorescence measurement (excitation  
104 485 nm, emission 535 nm,  $F_1$ ). In addition, the pellets were washed with 5 mM phosphate buffer once and  
105 then dissolved using 30 mM KCN to fully release the adsorbed FAM-DNA from the AuNPs. Similarly, 5  
106  $\mu\text{L}$  of the KCN treated solution was mixed with 95  $\mu\text{L}$  5mM pH 7.5 phosphate buffer for fluorescence  
107 measurement ( $F_2$ ). The fraction of DNA adsorption was determined by  $F_2/(F_1+F_2)$ .

## 108 AuNP-based binding assays

109 For the AuNP-based binding assays, different concentration ethanolamine (up to 2 mM), 35  $\mu$ L BB2 and  
110 50 nM aptamer EA# 14.3K42 were incubated for 1 min and then 5 nM AuNPs were added. After incubation  
111 for 10 min (total volume 100  $\mu$ L), the UV-vis absorption spectra of the samples were collected. The  
112 extinction ratio ( $A_{630}/A_{620}$ ) was calculated to determine the degree of aggregation. For the aptamer EA-  
113 Const and C-EA-Const, the process was the same except that 25  $\mu$ L BB2 was used in the system (total  
114 sample volume 100  $\mu$ L). A smaller volume of BB2 was used to achieve the optimal ionic strength for these  
115 two shorter aptamer sequences.

116

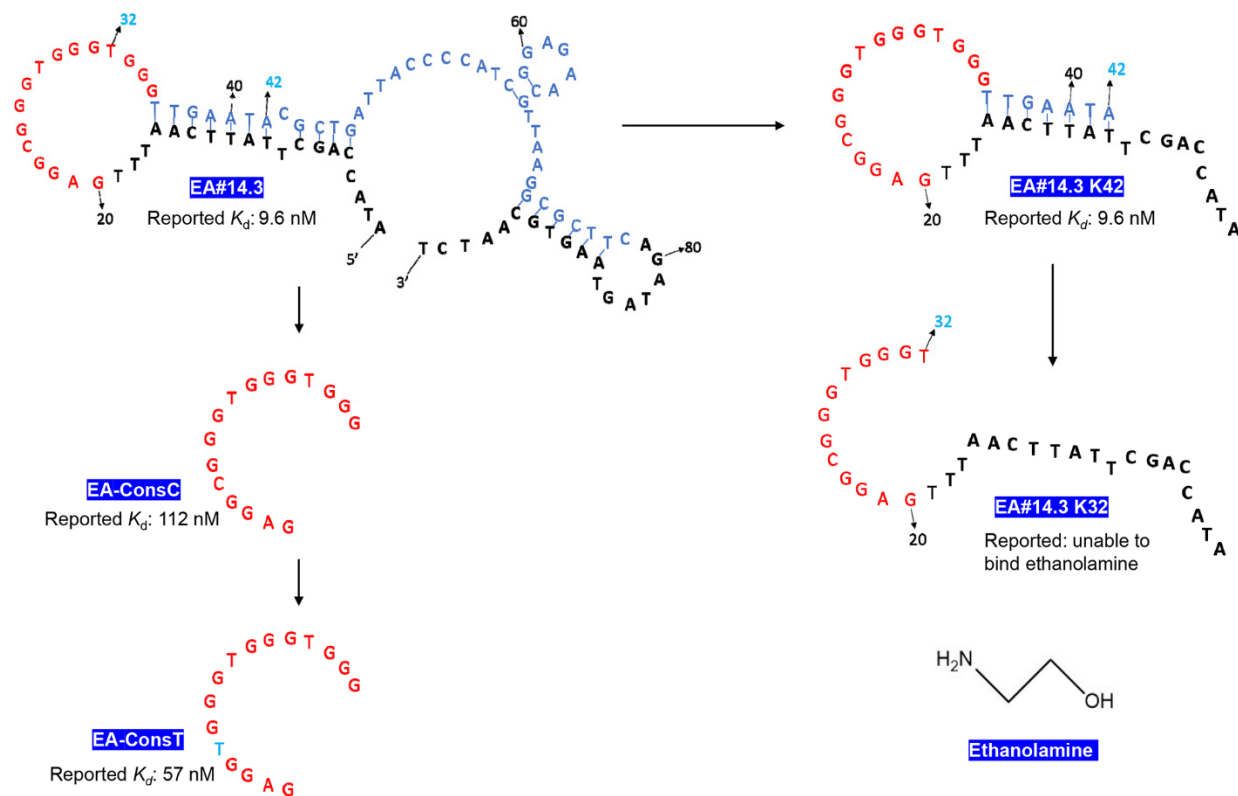
## 117 Results and Discussion

### 118 The ethanolamine aptamers

119 In the original aptamer selection paper, the authors organized their sequences into three groups, and they  
120 all share a common feature of having a guanine-rich segment towards the 5'-side of the random region.<sup>15</sup>  
121 Within each group, the sequences were well aligned. Two sequences (EA#14.3 and EA#9.4) were studied  
122 in detail and they actually had the same conserved guanine-rich region. Thus, we focused our study on  
123 EA#14.3, since its full-length aptamer was reported to have a 1-fold lower  $K_d$  compared to EA#9.4.<sup>16</sup>

124 The predicted secondary structure of the full-length 96-mer EA#14.3 is shown in Figure 1, and the  
125 two primer binding regions are shown in black. The guanine-rich region is shown in red, and the rest of the  
126 nucleotides are shown in blue. Truncation of all the nucleotides beyond A<sub>42</sub> resulted in the 42-mer  
127 EA#14.3K42 sequence, and the binding affinity was retained. Further truncation of it to a 32-mer sequence  
128 (EA#14.3K32) fully lost the binding, and it was attributed to the removal of the three guanines in the  
129 conserved guanine-rich region. When only the guanine-rich region was tested (named EA-ConsC), the  $K_d$   
130 was 112 nM. By mutating a single C in this EA-ConsC sequence to a thymine resulted in EA-Const with  
131 a lower 57 nM  $K_d$ . A 57 nM  $K_d$  still indicates a very good aptamer, since few small molecule binding DNA  
132 aptamers can reach such a low  $K_d$ . Based on previous studies, EA#14.3K42 and EA-Const were supposed  
133 to bind ethanolamine, but EA#14.3K32 could not bind. We included these three sequences in our study.

134 All these  $K_d$  values were measured by incubation of fluorescein-labeled aptamers with  
135 ethanolamine-modified beads in a way similar to aptamer selection. For such assays, there is a possibility  
136 of measurement of aptamer adsorption instead of specific binding. Therefore, in this work, we used  
137 homogenous binding assays free of immobilization.



138

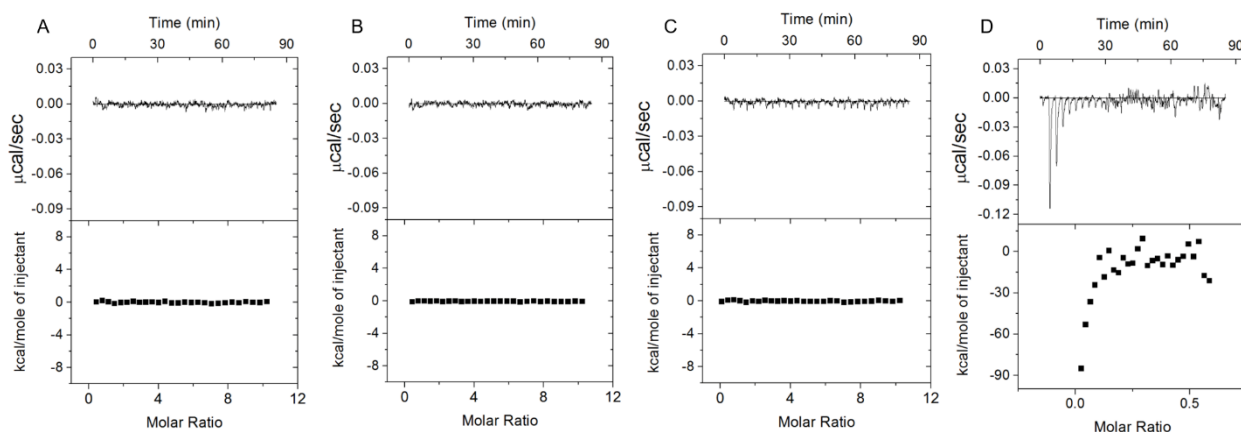
139 **Figure 1.** The secondary structure of the full-length 96-mer EA#14.3 aptamer and its truncated sequences used in this  
 140 study. The primer binding regions are in black and the library region is in red and blue. The reported  $K_d$  values are  
 141 taken from the literature.<sup>16</sup> The structure of ethanolamine is also shown.

142

### 143 Ethanolamine cannot bind with the aptamers using ITC

144 To directly measure the affinity between ethanolamine and the aptamers, we used ITC. ITC is a label-free  
 145 homogeneous technique allowing the extraction of all the thermodynamic parameters including dissociation  
 146 constant ( $K_d$ ).<sup>41, 42</sup> A lower  $K_d$  indicates stronger binding. From a previous study based on the immobilized  
 147 target,<sup>16</sup> the  $K_d$  of EA#14.3 was in the 9.4 nM to 18.6 nM range and the  $K_d$  of EA-Const was 57.3 nM.  $K_d$   
 148 in this range should be accurately measured by ITC. We titrated ethanolamine into the aptamers  
 149 (EA#14.3K42, EA#14.3K32 or EA-Const). However, no heat change was observed for any of the aptamers  
 150 (Figure 2A-C). We then did a control experiment by titrating the complementary DNA of EA-Const into  
 151 2  $\mu$ M EA-Const aptamer, and in this case heat was detected (Figure 2D). Therefore, ITC did not support  
 152 binding of ethanolamine by any of these three aptamers.<sup>16</sup> Interestingly, we noticed that the cDNA  
 153 hybridization to the DNA did not saturate at 1:1 but only a fraction of the DNA hybridized. We also raised  
 154 the concentration of the complementary DNA and even earlier saturation was observed (Figure S1). This  
 155 could be attributed to the potential secondary structures of the guanine-rich EA-Const and the cytosine-

156 rich complementary DNA, and they may form stable secondary structures on their own. Without an  
157 annealing process, only a fraction of unfolded DNA could hybridize.



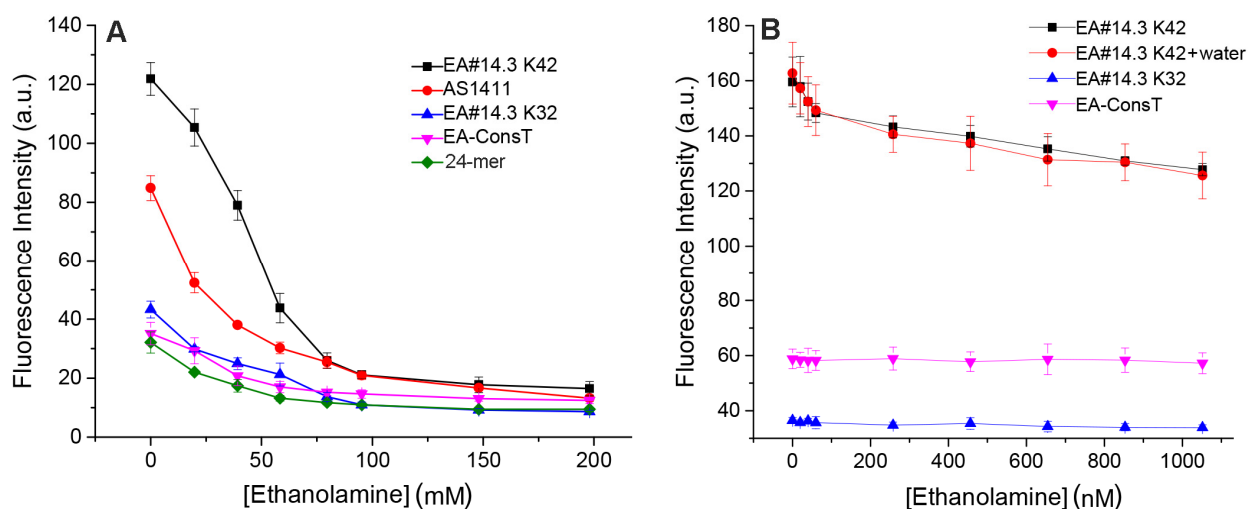
158  
159 **Figure 2.** ITC analysis of aptamer binding by titrating 200  $\mu\text{M}$  ethanolamine into 5  $\mu\text{M}$  (A) EA#14.3K42, (B)  
160 EA#14.3K32, and (C) EA-ConsT aptamers. (D) Titration of 5.72  $\mu\text{M}$  complementary DNA (C-EA-ConsT) into 2  $\mu\text{M}$   
161 EA-ConsT.

### 162 163 **ThT fluorescence spectroscopy indicating quenching instead of ethanolamine binding**

164 We then used fluorescence spectroscopy to perform homogeneous binding assays. Thioflavin T (ThT) is  
165 almost nonfluorescent on its own but it could generate a high fluorescence intensity when it is associated  
166 with G-quadruplex DNA.<sup>43</sup> Since the conserved region of the aptamer contains a guanine-rich sequence, a  
167 recent work used ThT to develop a label-free sensor for ethanolamine.<sup>28</sup> We herein repeated this experiment.  
168 We respectively mixed the aptamers (EA#14.3K42, EA#14.3K32 or EA-ConsT) with ThT and then  
169 gradually titrated ethanolamine. With 425 nm excitation, the emissions at 492 nm were monitored. As  
170 reported in the literature,<sup>28</sup> the fluorescence intensity of the samples decreased by gradually adding  
171 ethanolamine, and the middle point of the quenching curves was around 30-50 mM ethanolamine (Figure  
172 3A). This would suggest an apparent  $K_d$  of  $\sim 10^6$ -fold higher than previously reported.<sup>16</sup> We also tested two  
173 control DNA sequences, a 26-mer guanine-rich DNA (AS1411), and a 24-mer random sequenced DNA.  
174 They also showed a similar fluorescence quenching by ethanolamine (Figure 3A). In general, the initial  
175 fluorescence intensity was higher with a longer DNA containing more guanines (Figure S2), but they all  
176 showed a similar quenching profile.

177 To further confirm our results, we then titrated ethanolamine in the nM regions (up to 1  $\mu\text{M}$ ). If the  
178  $K_d$  values were less than 0.1  $\mu\text{M}$ , 1  $\mu\text{M}$  ethanolamine should be sufficient to saturate the binding. Typically,  
179 aptamer binding is expected to affect folding of aptamers,<sup>44</sup> which can be probed by a change in the

180 fluorescence of a DNA staining dye such as SYBR Green I and ThT.<sup>45-47</sup> However, no fluorescence change  
 181 was observed for EA-ConsT (supposed to bind) or EA#14.3K32 (not supposed to bind) (Figure 3B).  
 182 Although fluorescence dropping was observed for the EA#14.3K42 sample, we found that adding water  
 183 resulted in the same change. In fact, even just agitating the sample without anything also resulted in a  
 184 similar fluorescence drop (Figure S3). We reason that EA#14.3K42 has a large fraction of nucleotides in  
 185 the duplex state and its binding to ThT was unstable and perturbation by sample addition and agitation  
 186 could decrease the fluorescence. Therefore, this ThT fluorescence spectroscopy experiment did not support  
 187 specific aptamer binding. We reason that the observed quenching with mM ethanolamine was not due to  
 188 aptamer binding but due to ethanolamine serving as a fluorescence quencher, since amines are known  
 189 fluorescence quenchers.<sup>48</sup>



190  
 191 **Figure 3.** ThT fluorescence intensity at 492 nm from the ThT/DNA samples in the presence of different concentrations  
 192 of ethanolamine (A) up to 200 mM, and (B) up to 1  $\mu$ M. In (B), #EA14.3K42 + water means titrating the same volumes  
 193 of water into the system in place of ethanolamine.

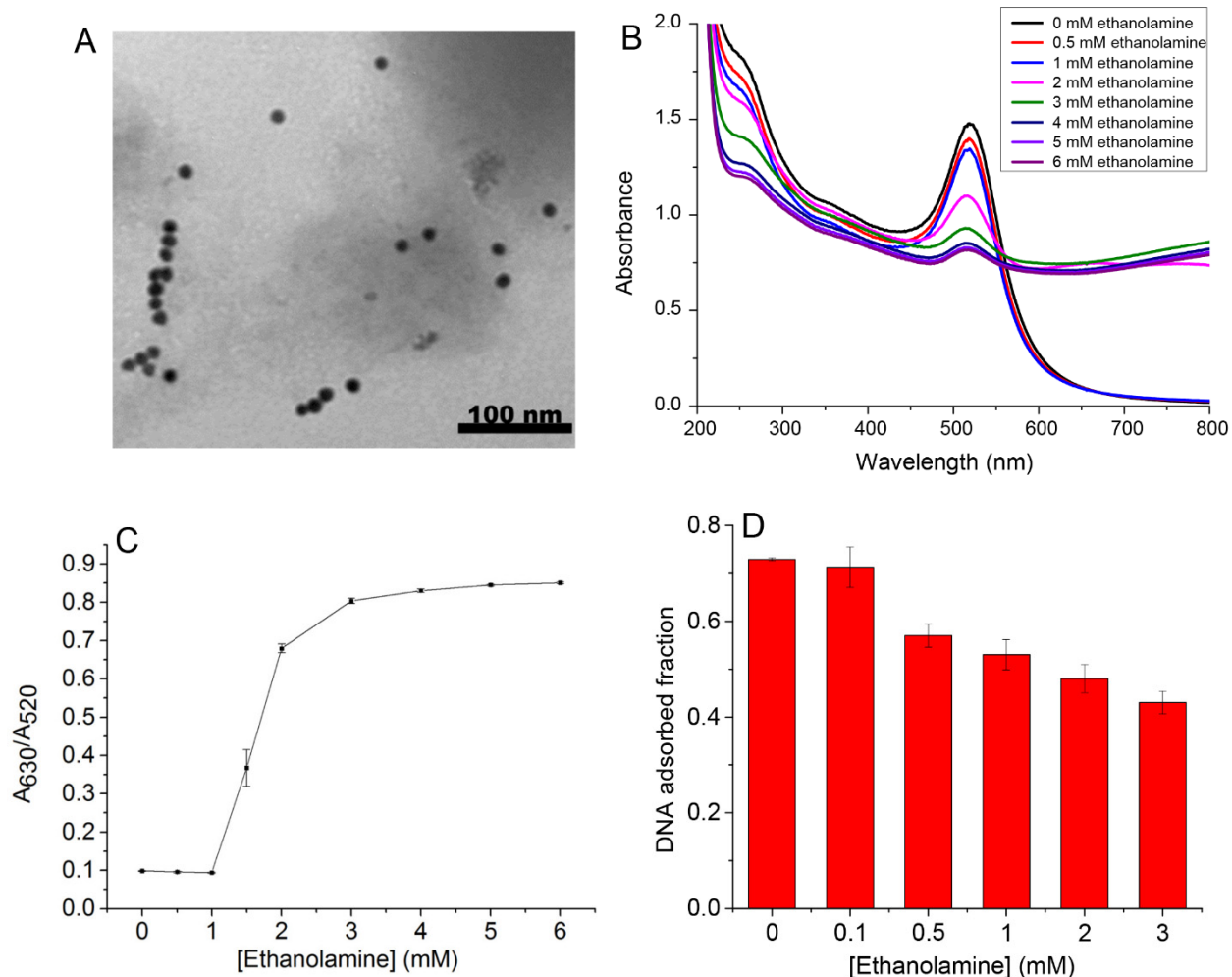
194  
 195 **Adsorption of ethanolamine to AuNPs: feasibility of the colorimetric binding assay**

196 Since homogeneous binding assays by ITC and ThT failed to support specific aptamer binding, we then  
 197 used AuNPs to do further tests. For such an assay, the assumption is that free aptamers can quickly adsorb  
 198 to AuNPs to increase their colloidal stability against salt-induced aggregation, whereas formation of an  
 199 aptamer/ethanolamine binding complex would slow down aptamer adsorption, leading to AuNP  
 200 aggregation and a red-to-blue color change upon adding salt.<sup>49, 50</sup> We recently emphasized that for such an  
 201 experiment to work as expected, the target analyte (ethanolamine in this case) cannot strongly adsorb to  
 202 AuNPs. Otherwise, the adsorbed target analyte can affect the colloidal stability of AuNPs and can also

203 inhibit DNA adsorption.<sup>25, 26</sup> Therefore, before performing this AuNP-based assay, we need to first  
204 understand the interaction between ethanolamine and AuNPs.

205 A TEM micrograph of our AuNP sample is shown in Figure 1A and they have an average diameter  
206 of 13 nm. After adding different concentrations of ethanolamine (up to 5 mM) into the citrate-capped  
207 AuNPs and incubation 1 min, the UV-vis spectra of the samples were collected (Figure 4B). The free  
208 AuNPs had a strong absorption peak at 520 nm, whereas upon adding a high concentration of ethanolamine,  
209 the AuNPs aggregated with the absorption in the 630 nm region increased. Therefore, we used the ratio of  
210 these two wavelengths to quantify the aggregation state of the AuNPs, with a higher ratio indicating  
211 aggregated AuNPs. As shown in Figure 4C, in the low concentration of ethanolamine (less than 1 mM), the  
212 AuNPs retained their colloidal stability. After adding more than 1 mM ethanolamine into the AuNPs, the  
213 AuNPs starts to aggregate, and they fully aggregated at 3 mM. Amines are known to adsorb to AuNPs via  
214 coordination of its lone pair electrons, although the affinity is much weaker compared to thiol.<sup>51</sup> The  
215 adsorbed ethanolamine would not contribute to charge stabilization since the exposed –OH group is non-  
216 charged. Thus, it is not surprising that high concentrations of ethanolamine could decrease the colloidal  
217 stability, since they might displace a fraction of the negatively charged citrate ligands. Compared to many  
218 other molecules with multiple metal binding ligands that can induce the aggregation of AuNPs at low  $\mu\text{M}$   
219 concentrations such as kanamycin,<sup>52</sup> dopamine and melamine,<sup>26</sup> and adenosine,<sup>45</sup> the single amine group in  
220 ethanolamine has much lower affinity to gold.

221 We then studied whether ethanolamine can influence the adsorption of DNA. We incubated AuNPs  
222 and a FAM-labeled DNA in the presence of different concentrations of ethanolamine (up to 3 mM) for 10  
223 min, and 50 mM NaCl was added to promote DNA adsorption.<sup>53</sup> The fraction of adsorbed DNA was  
224 quantified (Figure 4D), which was not much affected by  $<0.1$  mM ethanolamine. Considering the claimed  
225  $K_d$  of less than  $0.1 \mu\text{M}$ , the effect of ethanolamine on the stability of AuNPs and the adsorption of DNA is  
226 minimal and thus AuNPs might be a useful probe to study aptamer binding to ethanolamine.

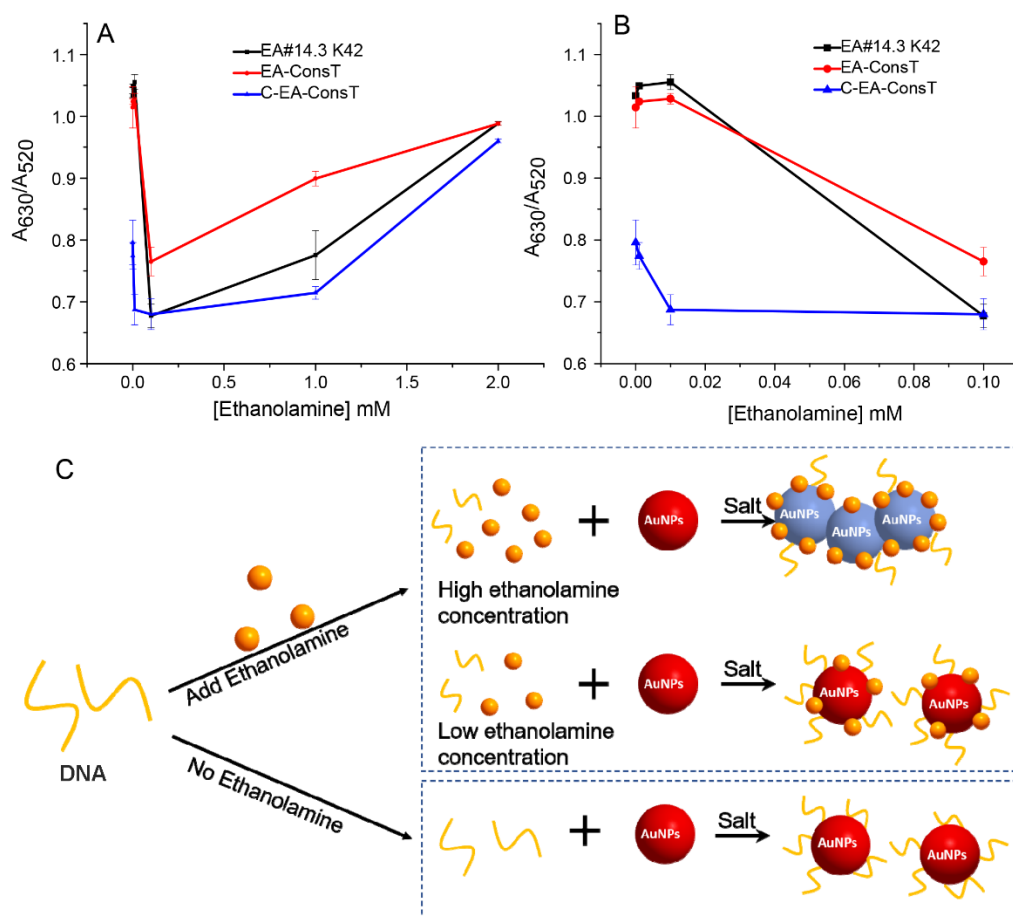


227  
 228 **Figure 4.** (A) A TEM micrograph of the 13 nm AuNPs. (B) UV-vis spectra of AuNPs incubated with various  
 229 concentrations of ethanolamine. (C) The absorbance ratio indicative of the colloidal stability of AuNPs by adding  
 230 different concentration ethanolamine. (D) The influence of ethanolamine on DNA adsorption on AuNPs calculated  
 231 after dissolving AuNPs by KCN.

232  
 233 **Homogeneous assays using AuNPs.**

234 We then performed the AuNP-based binding assay by adding AuNPs to the mixtures of aptamers and  
 235 ethanolamine. To avoid interference of HEPES buffer and surfactant, we prepared another binding buffer  
 236 (BB2), where HEPES was replaced by phosphate and Tween 20 was removed.<sup>54</sup> Since BB2 already  
 237 contained a high concentration of salt, no extra salt was added after mixing AuNPs with aptamers and  
 238 ethanolamine. The absorption ratio as a function of ethanolamine concentration was plotted (Figure 5A).  
 239 For the three sequences, only two were reported to bind ethanolamine, and C-EA-ConsT cannot bind.  
 240 However, all of the three sequences showed the same trend and we can separate our discussion in two

241 concentration regions. With low concentrations of ethanolamine (below 0.1 mM), the extinction ratio  
 242 decreased with increase of ethanolamine concentration indicating increased AuNPs stability. The low  
 243 concentration region responses are plotted in Figure 5B. If the ethanolamine could specifically bind with  
 244 certain aptamers in nanomolar range and such binding can inhibit aptamer adsorption, the AuNPs would  
 245 gradually aggregate after increasing the concentration of ethanolamine. However, we observed the opposite  
 246 with less than 0.1 mM ethanolamine. Thus, our results did not support the proposed mechanism and cannot  
 247 support specific aptamer binding. Since when the concentration of ethanolamine was below 0.1 mM, it did  
 248 not affect DNA adsorption (Figure 4C), we reason that the stabilization of AuNPs at lower than 0.1 mM  
 249 ethanolamine was due to ethanolamine serving as a competitive backfilling agent to force some DNA  
 250 strands to adopt an upright conformation. We previously observed such an effect with Br<sup>-</sup>.<sup>55</sup>



251  
 252 **Figure 5.** The absorbance ratio from the AuNP-based binding assays by incubation different aptamers with different  
 253 concentrations of ethanolamine (A) from 0 to 2 mM; and (B) from 0 to 0.1 mM. (C) Scheme showing the interaction  
 254 between ethanolamine, aptamers and AuNPs. Low concentration of ethanolamine (<0.1 mM) can slightly promote  
 255 AuNP stability, while high concentration of ethanolamine (>0.1 mM) inhibited DNA adsorption and decreased the  
 256 colloidal stability of AuNPs.

257

258 With higher than 0.1 mM ethanolamine, the stability of the AuNPs decreased with increase of  
259 ethanolamine concentration. At higher than 0.5 mM ethanolamine, the destabilization trend can be simply  
260 explained by the adsorption of ethanolamine inhibiting DNA adsorption as observed in Figure 4D and by  
261 ethanolamine-induced aggregation (Figure 4C). We summarized the effect of ethanolamine on AuNPs in  
262 Figure 5C.

## 263 Discussion

264 Taking all the three homogenous assays together, there is no evidence to support ethanolamine binding to  
265 the aptamers. We reason that the previously observed binding might be due to adsorption of the aptamers  
266 since most of them used immobilized ethanolamine.<sup>16,20</sup> The linker between ethanolamine and the materials  
267 for immobilization might also be involved in the binding. Therefore, such assays cannot support binding of  
268 free ethanolamine molecules.

269 For the published homogeneous assays, we already discussed the ThT based assay in Figure 3.<sup>28</sup>  
270 The only other homogenous binding assay measured the effect of ethanolamine on the melting temperature  
271 ( $T_m$ ) change of the aptamers.<sup>29</sup> The aptamers were labeled with a fluorophore and a quencher on the two  
272 ends and melting was followed by the fluorescence intensity. A close examination of the data suggested  
273 that the measured  $T_m$  might not be related to specific ethanolamine binding. For example, 0.5  $\mu$ M aptamer  
274 was used, but the change of  $T_m$  saturated at 0.1  $\mu$ M ethanolamine. In addition, a similar increase in  $T_m$  was  
275 observed for EA#14.3k42 at 1  $\mu$ M phenylethylamine, ethanol and propylamine, and based on the  $T_m$  value  
276 change, the  $K_d$  values for these three compounds were similar and below 5  $\mu$ M. These are vastly different  
277 molecules as aptamer targets and very unlikely that any aptamer can bind all of them with low micromolar  
278 affinity. Thus, we believe the measured  $T_m$  changes might be related to other factors than aptamer binding.  
279 In our study using three different homogenous binding assays, all the tested sequences behaved similarly  
280 regardless they were previously reported to bind ethanolamine or not. This study indicates the importance  
281 of using control sequences and multiple different assays to confirm aptamer binding,<sup>36,37</sup> and especially the  
282 importance of using homogeneous assays for studying free target molecules.

## 283 Conclusions

284 In conclusion, we performed three homogeneous assays using free ethanolamine and free aptamers  
285 including ITC, ThT fluorescence spectroscopy and AuNP-based colorimetry. However, we did not observe  
286 any evidence supporting specific aptamer binding to ethanolamine. The ThT fluorescence response in the  
287 mM ethanolamine range was attributed to ethanolamine acting as a quencher. In addition, we also studied  
288 the interaction between ethanolamine and AuNPs. When the concentration of ethanolamine is below 0.1

289 mM, AuNPs could serve as a useful probe for studying the binding between ethanolamine and its aptamers.  
290 It needs to be noted that we cannot rule out binding of these DNA sequences to the immobilized  
291 ethanolamine (with the linker and surfaces), but such binding is less relevant to the detection of biologically  
292 important free ethanolamine. Since many small molecule binding aptamers were isolated using immobilized  
293 targets, similar heterogeneous assays were also used to confirm their binding. This work articulates the  
294 importance of careful homogeneous binding assays using free target molecules.

295

## 296 **Acknowledgements**

297 Funding for this work was from a Mitacs Accelerate grant and from the Natural Sciences and Engineering  
298 Research Council of Canada (NSERC).

299

## 300 **References**

- 301 1. Y. Bai, C. Xiong, X. Shang and Y. Xin, *Energy & Fuels*, 2014, **28**, 1829-1837.
- 302 2. G. T. Rochelle, *Science*, 2009, **325**, 1652-1654.
- 303 3. S. B. Hawthorne, A. Kubátová, J. R. Gallagher, J. A. Sorensen and D. J. Miller, *Environ. Sci.*  
304 *Technol.*, 2005, **39**, 3639-3645.
- 305 4. D. Patel and S. N. Witt, *Oxidative Medicine and Cellular Longevity*, 2017, **2017**, 4829180.
- 306 5. K. G. Kaval, D. A. Garsin and V. Sperandio, *mBio*, 2018, **9**, e00066-00018.
- 307 6. V. M. Rivilla, I. Jiménez-Serra, J. Martín-Pintado, C. Briones, L. F. Rodríguez-Almeida, F. Rico-  
308 Villas, B. Tercero, S. Zeng, L. Colzi, P. de Vicente, S. Martín and M. A. Requena-Torres, *Proc.*  
309 *Natl. Acad. Sci. USA*, 2021, **118**, e2101314118.
- 310 7. M. J. Ormsby, M. Logan, S. A. Johnson, A. McIntosh, G. Fallata, R. Papadopoulou, E. Papachristou,  
311 G. L. Hold, R. Hansen, U. Z. Ijaz, R. K. Russell, K. Gerasimidis and D. M. Wall, *EBioMedicine*,  
312 2019, **43**, 325-332.
- 313 8. X. Q. Su, J. Wang and A. J. Sinclair, *Lipids in Health and Disease*, 2019, **18**, 100.
- 314 9. O. Mrklas, A. Chu and S. Lunn, *J. Environ. Monit.*, 2003, **5**, 336-340.
- 315 10. B. Sikarwar, P. K. Sharma, B. K. Tripathi, M. Boopathi, B. Singh and Y. K. Jaiswal,  
316 *Electroanalysis*, 2016, **28**, 881-889.
- 317 11. A. Ruscito and M. C. DeRosa, *Front. Chem.*, 2016, **4**, 14.
- 318 12. O. Alkhamis, J. Canoura, H. X. Yu, Y. Z. Liu and Y. Xiao, *TrAC-Trends Anal. Chem.*, 2019, **121**,  
319 115699.

- 320 13. H. Yu, O. Alkhamis, J. Canoura, Y. Liu and Y. Xiao, *Angew. Chem. Int. Ed.*, 2021, **60**, 16800-  
321 16823.
- 322 14. N. Nakatsuka, K.-A. Yang, J. M. Abendroth, K. M. Cheung, X. Xu, H. Yang, C. Zhao, B. Zhu, Y.  
323 S. Rim, Y. Yang, P. S. Weiss, M. N. Stojanović and A. M. Andrews, *Science*, 2018, **362**, 319-324.
- 324 15. D. Mann, C. Reinemann, R. Stoltenburg and B. Strehlitz, *Biochem. Biophys. Res. Commun.*, 2005,  
325 **338**, 1928.
- 326 16. A. Heilkenbrinker, C. Reinemann, R. Stoltenburg, J.-G. Walter, A. Jochums, F. Stahl, S.  
327 Zimmermann, B. Strehlitz and T. Scheper, *Anal. Chem.*, 2015, **87**, 677-685.
- 328 17. D. E. Huizenga and J. W. Szostak, *Biochemistry*, 1995, **34**, 656-665.
- 329 18. O. Oni, Z. Zhang and J. Liu, *Nucleic Acids Res.*, 2017, **45**, 7593-7601.
- 330 19. X. Liu, Y. Hou, S. Chen and J. Liu, *Biosens. Bioelectron.*, 2020, 112798.
- 331 20. C. Reinemann, R. Stoltenburg and B. Strehlitz, *Anal. Chem.*, 2009, **81**, 3973-3978.
- 332 21. C.-Y. Lee, R.-J. Shiau, H.-W. Chou and Y.-Z. Hsieh, *Sensors Actuat. B: Chem.*, 2018, **254**, 189-  
333 196.
- 334 22. Z. Khoshbin, J. Zamanian, N. Davoodian, N. Mohammad Danesh, M. Ramezani, M. Alibolandi,  
335 K. Abnous and S. M. Taghdisi, *Spectrochimica Acta A*, 2022, **267**, 120488.
- 336 23. M. Mahmoud, S. Laufer and H. P. Deigner, *Microchimica Acta*, 2019, **186**.
- 337 24. G. Liang, Y. Man, X. X. Jin, L. G. Pan and X. H. Liu, *Anal. Chim. Acta*, 2016, **936**, 222-228.
- 338 25. F. Zhang and J. Liu, *Anal. Sens.*, 2021, **1**, 30-43.
- 339 26. X. Liu, F. He, F. Zhang, Z. Zhang, Z. Huang and J. Liu, *Anal. Chem.*, 2020, **92**, 9370-9378.
- 340 27. A. Lopez and J. Liu, *Anal. Chem.*, 2021, **93**, 3018-3025.
- 341 28. A. T. Bayraç and Y. Acar, *Dyes and Pigments*, 2020, **172**, 107788.
- 342 29. M. Mahmoud, S. Laufer and H.-P. Deigner, *Biochimie*, 2019, **158**, 233-237.
- 343 30. C. Zong and J. Liu, *Anal. Chem.*, 2019, **91**, 10887-10893.
- 344 31. F. Bottari, E. Daems, A.-M. de Vries, P. Van Wielendaele, S. Trashin, R. Blust, F. Sobott, A.  
345 Madder, J. C. Martins and K. De Wael, *J. Am. Chem. Soc.*, 2020, **142**, 19622-19630.
- 346 32. L. Zara, S. Achilli, B. Chovelon, E. Fiore, J.-J. Toulmé, E. Peyrin and C. Ravelet, *Anal. Chim. Acta*,  
347 2021, **1159**, 338382.
- 348 33. I. Álvarez-Martos and E. E. Ferapontova, *Biochem. Biophys. Res. Commun.*, 2017, **489**, 381-385.
- 349 34. Y. Hou, J. Hou and X. Liu, *ChemBioChem*, 2021, **22**, 1948-1954.
- 350 35. X. Tao, F. He, X. Liu, F. Zhang, X. Wang, Y. Peng and J. Liu, *Microchimica Acta*, 2020, **187**, 668.
- 351 36. Y. Zhao, K. Yavari and J. Liu, *TrAC-Trends Anal. Chem.*, 2022, 116480.
- 352 37. E. Daems, G. Moro, R. Campos and K. De Wael, *TrAC-Trends Anal. Chem.*, 2021, **142**, 116311.

- 353 38. M. McKeague, A. De Girolamo, S. Valenzano, M. Pascale, A. Ruscito, R. Velu, N. R. Frost, K.  
354 Hill, M. Smith, E. M. McConnell and M. C. DeRosa, *Anal. Chem.*, 2015, **87**, 8608-8612.
- 355 39. J. Liu and Y. Lu, *Nature Protocols*, 2006, **1**, 246-252.
- 356 40. J. Turkevich, P. C. Stevenson and J. Hillier, *Discussions of the Faraday Society*, 1951, **11**, 55-75.
- 357 41. S. Slavkovic, Y. Zhu, Z. R. Churcher, A. A. Shoara, A. E. Johnson and P. E. Johnson, *Sci. Rep.*,  
358 2020, **10**, 18944.
- 359 42. S. Slavkovic and P. E. Johnson, *Aptamers*, 2018, **2**, 45-51.
- 360 43. F. Y. Khusbu, X. Zhou, H. Chen, C. Ma and K. Wang, *TrAC-Trends Anal. Chem.*, 2018, **109**, 1-18.
- 361 44. T. Hermann and D. J. Patel, *Science*, 2000, **287**, 820-825.
- 362 45. F. Zhang, P.-J. J. Huang and J. Liu, *ACS Sensors*, 2020, **5**, 2885–2893.
- 363 46. A. Renaud de la Faverie, A. Guédin, A. Bedrat, L. A. Yatsunyk and J.-L. Mergny, *Nucleic Acids*  
364 *Res.*, 2014, **42**, e65-e65.
- 365 47. M. McKeague, R. Velu, A. De Girolamo, S. Valenzano, M. Pascale, M. Smith and M. C. DeRosa,  
366 *Toxins*, 2016, **8**, 336.
- 367 48. S.-P. Van and G. S. Hammond, *J. Am. Chem. Soc.*, 1978, **100**, 3895-3902.
- 368 49. H. Li and L. J. Rothberg, *J. Am. Chem. Soc.*, 2004, **126**, 10958-10961.
- 369 50. H. Li and L. Rothberg, *Proc. Natl. Acad. Sci. USA*, 2004, **101**, 14036-14039.
- 370 51. R. C. Hoft, M. J. Ford, A. M. McDonagh and M. B. Cortie, *J. Phys. Chem. C*, 2007, **111**, 13886-  
371 13891.
- 372 52. J. Zhou, Y. Li, W. Wang, Z. Lu, H. Han and J. Liu, *Langmuir*, 2020, **36**, 11490–11498.
- 373 53. X. Zhang, M. R. Servos and J. Liu, *Langmuir*, 2012, **28**, 3896-3902.
- 374 54. P.-J. J. J. Huang, J. Yang, K. Chong, Q. Ma, M. Li, F. Zhang, W. J. Moon, G. Zhang and J. Liu,  
375 *Chem. Sci.*, 2020, **11**, 6795-6804.
- 376 55. B. Liu, P. Wu, Z. Huang, L. Ma and J. Liu, *J. Am. Chem. Soc.*, 2018, **140**, 4499–4502.

377

378